Precision GeoSurveys

AIRBORNE GEOPHYSICAL SURVEY REPORT

Mount Vic Survey Blocks

Carmacks, YT

Hill 79 Resources Corp.

Precision GeoSurveys Inc.
www.precisiongeosurveys.com
Hangar 42 Langley Airport
21330 - 56th Ave., Langley, BC
Canada V2Y 0E5
604-484-9402

Jenny Poon, B.Sc., P.Geo.

September 2020
Job# 20138

Table of Contents

List of Figures

List of Tables

List of Appendices

List of Mount Vic – North Plates (Scale 1:15,000)

Plate 1_N: Mount Vic - North – Actual Flight Lines (FL)
Plate 2_N: Mount Vic - North – Digital Terrain Model (DTM)
Plate 3_N: Mount Vic - North – Total Magnetic Intensity with Actual Flight Lines (TMI_wFL)
Plate 4_N: Mount Vic - North – Total Magnetic Intensity (TMI)
Plate 5_N: Mount Vic - North – Residual Magnetic Intensity (RMI)
Plate 6_N: Mount Vic - North – Reduced to Magnetic Pole (RTP) of RMI
Plate 7_N: Mount Vic - North – Calculated Horizontal Gradient (CHG) of RMI
Plate 8_N: Mount Vic - North – Calculated Vertical Gradient (CVG) of RMI
Plate 9_N: Mount Vic - North – Potassium - Percentage (%K)
Plate 10_N: Mount Vic - North – Thorium - Equivalent Concentration (eTh)
Plate 11_N: Mount Vic - North – Uranium - Equivalent Concentration (eU)
Plate 12_N: Mount Vic - North – Total Count (TC)
Plate 13_N: Mount Vic - North – Total Count - Exposure Rate (TCexp)
Plate 14_N: Mount Vic - North – Potassium over Thorium Ratio (%K/eTh)
Plate 15_N: Mount Vic - North – Potassium over Uranium Ratio (%K/eU)
Plate 16_N: Mount Vic - North – Uranium over Thorium Ratio (eU/eTh)
Plate 17_N: Mount Vic - North – Uranium over Potassium Ratio (eU/%K)
Plate 18_N: Mount Vic - North – Thorium over Potassium Ratio (eTh/%K)
Plate 19_N: Mount Vic - North – Thorium over Uranium Ratio (eTh/eU)
Plate 20_N: Mount Vic - North – Ternary Image (TI)

List of Mount Vic – South Plates (Scale 1:15,000)

Plate 1_S: Mount Vic - South – Actual Flight Lines (FL)
Plate 2_S: Mount Vic - South – Digital Terrain Model (DTM)
Plate 3_S: Mount Vic - South – Total Magnetic Intensity with Actual Flight Lines (TMI_wFL)
Plate 4_S: Mount Vic - South – Total Magnetic Intensity (TMI)
Plate 5_S: Mount Vic - South – Residual Magnetic Intensity (RMI)
Plate 6_S: Mount Vic - South – Reduced to Magnetic Pole (RTP) of RMI
Plate 7_S: Mount Vic - South – Calculated Horizontal Gradient (CHG) of RMI
Plate 8_S: Mount Vic - South – Calculated Vertical Gradient (CVG) of RMI
Plate 9_S: Mount Vic - South – Potassium - Percentage (%K)
Plate 10_S: Mount Vic - South – Thorium - Equivalent Concentration (eTh)
Plate 11_S: Mount Vic - South – Uranium - Equivalent Concentration (eU)
Plate 12_S: Mount Vic - South – Total Count (TC)
Plate 13_S: Mount Vic - South – Total Count - Exposure Rate (TCexp)
Plate 14_S: Mount Vic - South – Potassium over Thorium Ratio (%K/eTh)
Plate 15_S: Mount Vic - South – Potassium over Uranium Ratio (%K/eU)
Plate 16_S: Mount Vic - South – Uranium over Thorium Ratio (eU/eTh)
Plate 17_S: Mount Vic - South – Uranium over Potassium Ratio (eU/%K)
Plate 18_S: Mount Vic - South – Thorium over Potassium Ratio (eTh/%K)
Plate 19_S: Mount Vic - South – Thorium over Uranium Ratio (eTh/eU)
Plate 20_S: Mount Vic - South – Ternary Image (TI)

1.0 Introduction

This report outlines the geophysical survey operations and data processing procedures taken during the high resolution helicopter-borne aeromagnetic and radiometric survey flown over the North and South survey blocks at the Mount Vic mineral exploration project for Hill 79 Resources Corp. The survey blocks are located in southwestern Yukon (Figure 1) and were flown from August 6 to August 10, 2020.

Figure 1: Mount Vic survey area located in southwestern Yukon.

1.1 Survey Area

Mount Vic survey blocks are centered at Mount Victoria, approximately 47 km west of Carmacks, Yukon (Figure 2). A total of 864 line km of magnetic and radiometric data was collected over two survey blocks with a total area of 38.4 km^2.

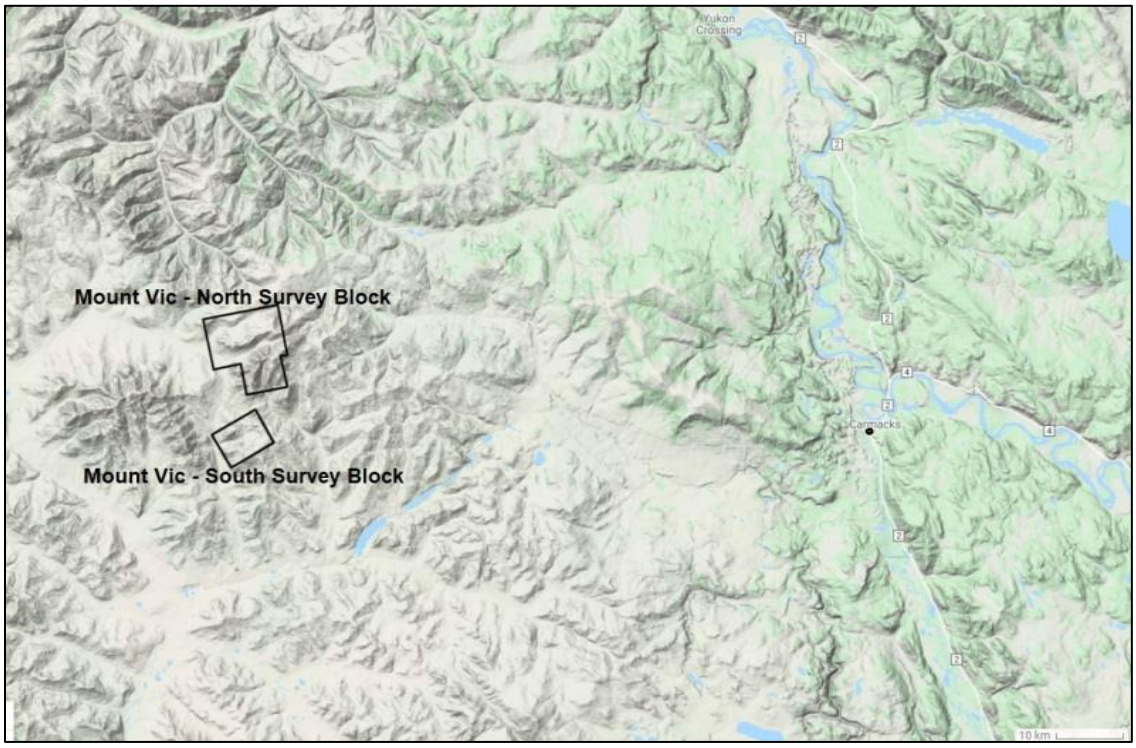

Figure 2: Mount Vic – North and South survey blocks west of Carmacks, Yukon.

The Mount Vic - North survey block with an area of 28.0 km^2 was flown at 50 m line spacing at a heading of 170°/350°; tie lines were flown at 500 m spacing at a heading of 080°/260° (Figures 3 and 4).

Figure 3: Plan View – Mount Vic - North survey block with actual flight lines in yellow and survey block boundary in white.

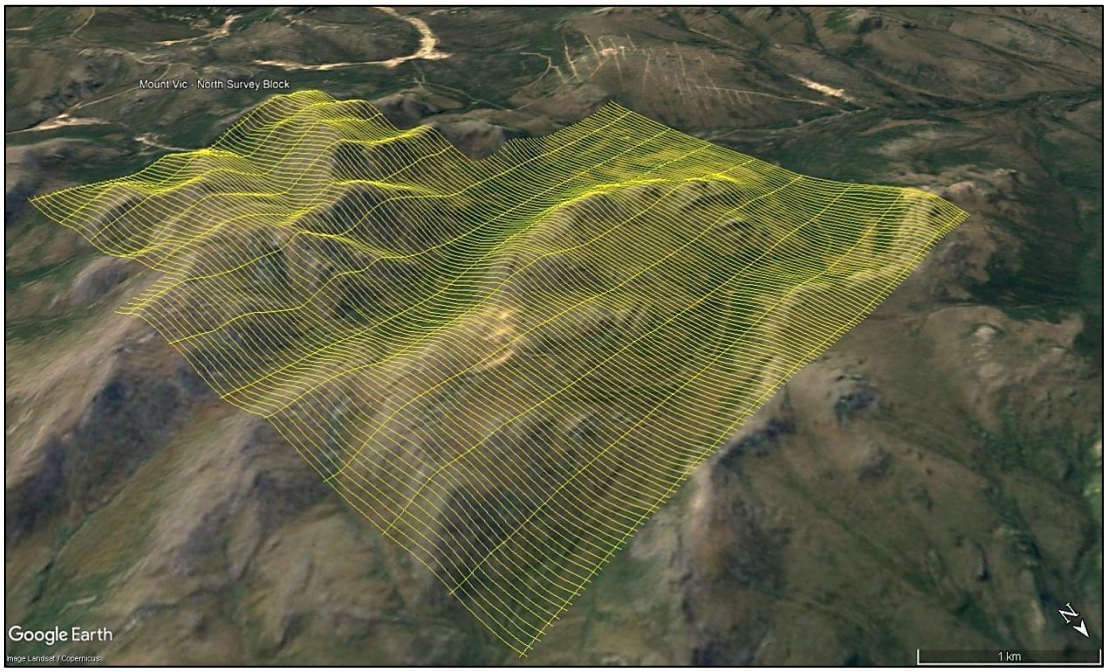

Figure 4: Terrain View – Mount Vic - North survey block with actual flight lines displayed in yellow.

The Mount Vic - South survey block with an area of 10.4 km^2 was flown at 50 m line spacing at a heading of 060°/240°; tie lines were flown at 500 m spacing at a heading of 150°/330° (Figures 5 and 6).

Figure 5: Plan View – Mount Vic - South survey block with actual flight lines in yellow and survey block boundary in white.

Figure 6: Terrain View – Mount Vic - South survey block with actual flight lines displayed in yellow.

1.2 Survey Specifications

The geodetic system used for the geophysical survey was WGS 84 in UTM Zone 8N. A total of 864 line km was flown (Table 1). Survey block polygon coordinates for Mount Vic – North and South are specified in Appendix A.

Mount Vic Survey Block	Area (km^2)	Line Type	No. of Lines Planned	No. of Lines Completed	Line Spacing (m)	Line Orientation (UTM grid)	Mean Survey Height (m)	Total Planned Line km	Total Actual km Flown
North	28.0	Survey	112	112	50	170°/350°	42.2	569	569
		Tie	13	13	500	080°/260°	42.5	60	60
		Total:	**125**	**125**			**42.2**	**629**	**629**
South	10.4	Survey	57	57	50	060°/240°	41.5	212	212
		Tie	8	8	500	150°/330°	42.2	23	23
		Total:	**65**	**65**			**41.6**	**235**	**235**
Total	**38.4**		**190**	**190**				**864**	**864**

Table 1: Survey flight line specifications.

2.0 Geophysical Data

Geophysical data are collected in a variety of ways and are used for many purposes including aiding in the determination of geology, mineral deposits, oil and gas deposits, geotechnical investigations, contaminated land sites, and UXO (unexploded ordnance) detection.

For the purposes of this survey, airborne magnetic and radiometric data were collected to serve in geological mapping and exploration for mineral deposits.

2.1 Magnetic Data

Magnetic surveying is the most common airborne geophysical technology used for both mineral and hydrocarbon exploration. Aeromagnetic surveys measure and record the total intensity of the magnetic field at the magnetometer sensor, which is a combination of the desired magnetic field generated in the Earth as well as small variations due to temporal effects of the constantly varying solar wind. By subtracting temporal and regional magnetic effects, the resulting aeromagnetic maps show the spatial distribution and relative abundance of magnetic minerals - most commonly the iron oxide mineral magnetite - in the upper levels of Earth's crust, which in turn are related to lithology, structure, and alteration of bedrock. Survey specifications, instrumentation, and interpretation procedures depend on the objectives of the survey. Magnetic surveys are typically performed for:

- Geological Mapping - to aid in mapping lithology, structure, and alteration.
- Depth to Basement Mapping - for exploration in sedimentary basins or mineralization associated with the basement surface.

2.2 Radiometric Data

Radiometric surveys are used to determine either the absolute or relative concentrations of uranium (U), thorium (Th), and potassium (K) in surface rocks and soils using natural radioactive emanations. Gamma radiation is utilized due to its greater penetration depth compared with alpha and beta radiation. Radiometric data are useful for mapping lithology, alteration, and structure as well as providing insights into weathering. For example, the natural radioactivity of igneous rocks generally increases with SiO_2 content and clay minerals tend to fix the natural radioelements.

Gamma rays are electromagnetic waves with frequencies between 10^{19} and 10^{21} Hz emitted spontaneously from an atomic nucleus during radioactive decay, in packets referred to as photons. The energy E transported by a photon is related to the wavelength λ or frequency ν by the formula:

$$E = h\nu = hc/\lambda$$

where: c is the velocity of light
h is Planck's constant (6.626×10^{-34} joule).

All detectable gamma radiation from Earth materials comes from the natural decay products of three primary radioelements: U, Th, and K. Each individual nuclear species (isotope) emits gamma rays at one or more specific energies, as shown in Figure 7. Of these elements, only potassium (^{40}K) emits gamma energy directly, at 1.46 MeV. Uranium (^{238}U) and thorium (^{232}Th) emit gamma rays through their respective decay series; ^{214}Bi at 1.76 MeV for uranium and ^{208}Tl at 2.61 MeV for thorium. Accordingly, the ^{214}Bi and ^{208}Tl measurements are considered equivalents for uranium (eU) and thorium (eTh), as the daughter products will be in equilibrium under most natural conditions.

Surficial debris, vegetation, standing water (lakes, marshes, swamps), and snow can effectively attenuate gamma rays originating from underlying rocks. Therefore, variations in isotope counts must be evaluated with respect to surficial conditions before they are attributed to changes in underlying geology. An increase in soil moisture can also significantly affect gamma radiation concentrations. For example, a 10% increase in soil moisture can decrease the measured gamma radiation by about the same amount. Radon isotopes are long-lived members of both the U and Th decay series and Ra mobility can influence radiometric surveys. In addition to being directly radioactive, ^{226}Ra and ^{222}Rn can attach to dust particles in the atmosphere. Radioactive precipitation of these dust particles by rain can lead to apparent increases of more than 2000% in uranium ground concentration (IAEA, 2003). Therefore, gamma data should not be collected during a rainfall, or shortly after a rainfall.

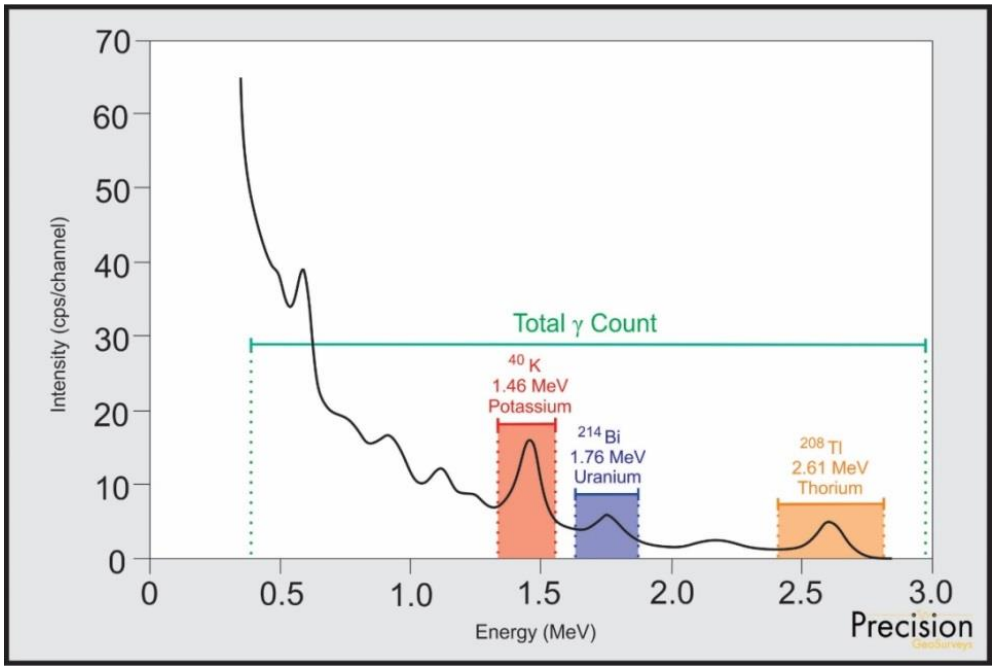

Figure 7: Typical natural gamma spectrum showing the three spectral windows (^{40}K 1.37-1.57 MeV, ^{214}Bi 1.66-1.86 MeV, ^{208}Tl 2.41-2.81 MeV) and total count (0.40-2.81 MeV) window.

3.0 Aircraft and Equipment

All geophysical and subsidiary equipment were carefully installed on the survey aircraft by Precision GeoSurveys to collect high resolution magnetic and radiometric data.

3.1 Aircraft

Precision GeoSurveys flew the survey using an Airbus AS350 helicopter, registration C-GSVY, at a nominal height of 40 m AGL.

3.2 Geophysical Equipment

The survey aircraft (Figure 8) was equipped with a magnetometer, spectrometer, data acquisition system, laser altimeter, fluxgate, barometer, temperature/humidity probe, pilot guidance unit (PGU), and GPS navigation system. In addition, two magnetic base stations were used to record temporal magnetic variations.

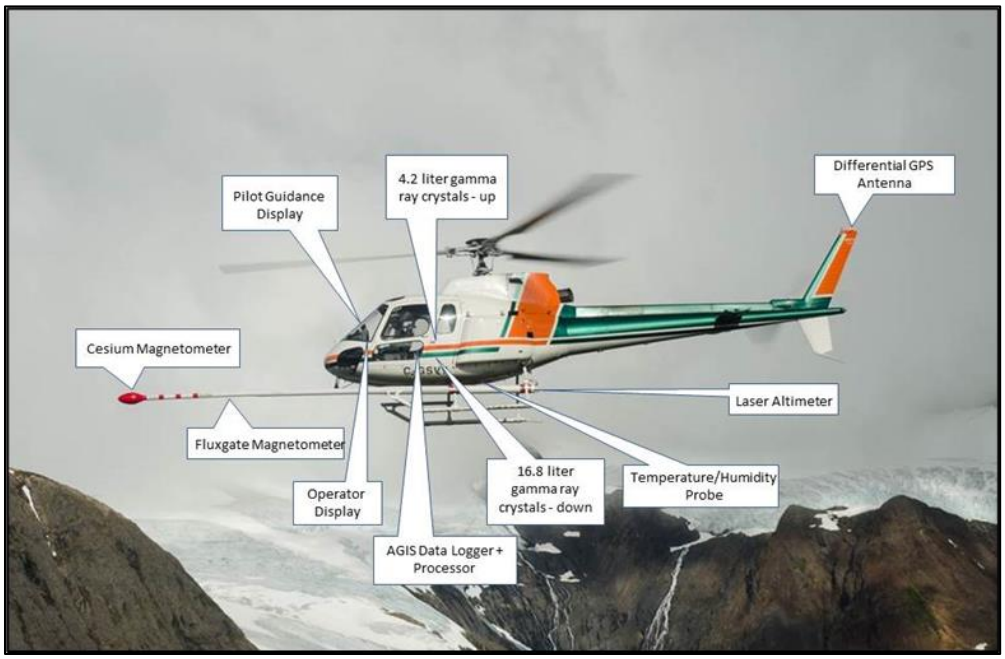

Figure 8: Airbus AS350 helicopter equipped with geophysical equipment.

3.2.1 Magnetometer

The survey was flown with a Scintrex CS-3 (Figure 9) split-beam cesium vapor magnetometer mounted on the front of the helicopter in a non-magnetic and non-conductive "stinger" configuration to measure total magnetic intensity. The CS-3 magnetometer (Figure 10) was orientated at 45 degrees from vertical to couple with local magnetic field.

Figure 9: View of CS-3 cesium vapor magnetometer.

Figure 10: View of "stinger" configuration. Cesium vapor magnetometer sensor orientated 45° from vertical to couple with local magnetic field.

3.2.2 Spectrometer

Gamma radiation data were collected by an Advanced Gamma Ray Spectrometer (AGRS-5) system manufactured by Nuvia Dynamics. The AGRS is an intelligent, self-calibrating, fully integrated gamma detection system (Figure 11) containing five thallium-activated synthetic sodium iodide crystals; 16.8 litres downward-looking and 4.2 litres upward-looking, with 256 channel output at 1 Hz sampling rate. The downward-looking crystals are designed to measure gamma rays from below the aircraft. The upward-looking crystal is mounted directly on top of the four downward-looking crystals to measure cosmic and solar gamma radiation originating

from above the survey aircraft and is shielded from terrestrial radiation by the downward-looking crystals. The AGRS system is installed in the rear passenger cabin of the helicopter away from the fuel tank to minimize variable gamma attenuation from fluctuating fuel levels.

Figure 11: AGRS-5 gamma spectrometer system with five detectors; a total of 21 litres NaI(Tl) synthetic crystals with 4 down and 1 up.

3.2.3 IMPAC

The Integrated Multi-Parameter Acquisition Console (IMPAC) (Figure 12), manufactured by Nuvia Dynamics Inc. (previously Pico Envirotec Inc.), is the main computer used in integrated data recording, data synchronizing, providing real-time quality control data for the geophysical operator display, and the generation of navigation information for the pilot and operator display systems.

Figure 12: IMPAC data acquisition and navigation system.

IMPAC uses the Microsoft Windows operating system and geophysical parameters are based on Nuvia's Airborne Geophysical Information System (AGIS) software. Depending on survey specifications, information such as magnetic field, electromagnetic data, total gamma count,

counts of various radioelements (K, U, Th, etc.), cosmic radiation, barometric pressure, atmospheric humidity, temperature, navigation parameters, and GPS status can all be monitored on the AGIS on-board display (Figure 13).

While in flight, raw magnetic response, magnetic fourth difference, compensated and uncompensated data, radiometric spectra, aircraft position, survey altitude, cross track error, and other parameters are recorded and can be viewed by the geophysical operator for immediate QC (quality control). Additional software allows for post or real time magnetic compensation and radiometric calibration.

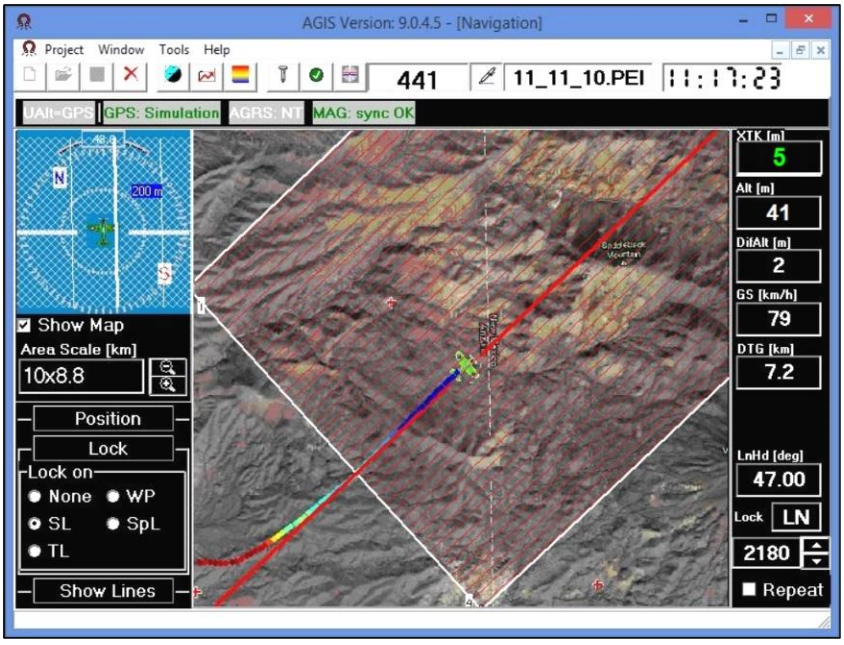

Figure 13: AGIS operator display, showing real time flight line recording and navigation parameters. Additional windows display real-time geophysical data to operator.

3.2.4 Magnetic Base Station

Temporal variations of Earth's magnetic field, particularly diurnal, are monitored and recorded by two GEM GSM-19T base station magnetometers. They were operated at all times while airborne data were being collected. The base stations were located in an area with low magnetic gradient, away from electric power transmission lines and moving ferrous objects, such as motor vehicles, that could affect the survey data integrity.

The GEM GSM-19T magnetometer (Figure 14) with integrated GPS time synchronization uses proton precession technology with absolute accuracy of ±0.20 nT and sensitivity of 0.15 nT at 1 Hz. Base station magnetic data were recorded on internal solid-state memory and downloaded onto a field laptop computer using a serial cable and GEMLink 5.4 software. Profile plots of the base station readings were generated, updated, and reviewed at the end of each survey day.

Figure 14: GEM GSM-19T proton precession magnetometer.

3.2.5 Fluxgate Magnetometer

As the survey aircraft flies along a survey line, small attitude changes (pitch, roll, and yaw) are recorded by a triaxial fluxgate magnetometer (Figure 15). The fluxgate consists of three magnetic sensors - X, Y, and Z - operating independently and simultaneously. Each sensor has an analog output corresponding to the component of the ambient magnetic field along its axis. Response of the sensors is proportional to the cosine of the angle between the applied field and the sensor's sensitive axis. Fluxgate data are used for magnetic compensation and attitude corrections.

Figure 15: Billingsley Triaxial fluxgate magnetometer.

3.2.6 Laser Altimeter

Terrain clearance is measured by an Opti-Logic RS800 Rangefinder laser altimeter (Figure 16) attached to the aft end of the magnetometer boom. The RS800 laser is a time-of-flight sensor that measures distance by a rapidly modulated and collimated laser beam that creates a dot on the target surface. The maximum range of the laser altimeter is 700 m off natural surfaces with accuracy of ±1 m on 1 x 1 m diffuse target with 50% (±20%) reflectivity. Within the sensor unit, reflected signal light is collected by the lens and focused onto a photodiode. Through serial communications and digital outputs, ground clearance data are transmitted to an RS-232 compatible port and recorded and displayed by the AGIS and PGU at 10 Hz in meters.

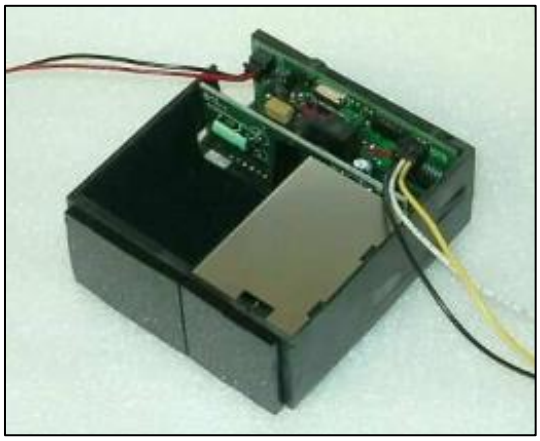

Figure 16: Opti-Logic RS800 Rangefinder laser altimeter.

3.2.7 Pilot Guidance Unit

Steering and elevation (ground clearance) information is continuously provided to the pilot by the Pilot Guidance Unit (PGU). The graphical display is mounted on top of the aircraft's instrument panel, remotely from the data acquisition system. The PGU is the primary navigation aid (Figure 17) to assist the pilot in keeping the aircraft on the planned flight path, heading, speed, and at the desired ground clearance.

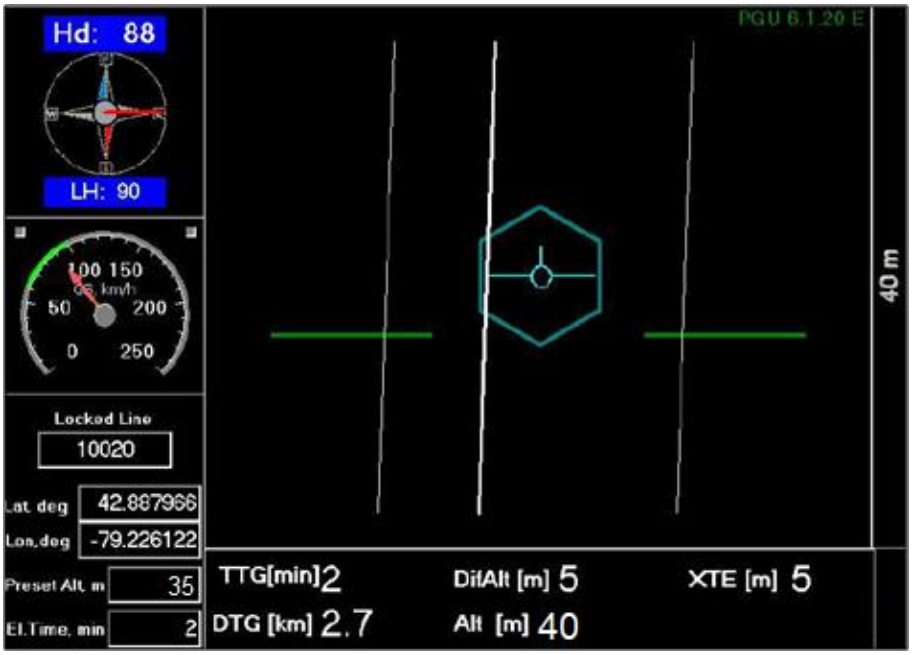

Figure 17: PGU screen displaying navigation information.

PGU information is displayed on a full VGA 600 x 800 pixel 7 inch (17.8 cm) LCD display. The CPU for the PGU is contained in a PC-104 console and uses Microsoft Windows operating system control, with input from the GPS antenna on the aircraft, laser altimeter, and AGIS.

3.2.8 GPS Navigation System

A Hemisphere R320 GPS receiver (Figure 18) and a Novatel GPS antenna on the aircraft integrated with the AGIS navigation system and pilot display (PGU) provide accurate navigational information and control. The R320 GPS receiver supports fast updates at a rate of up to 20 Hz (20 times per second); delivering sub-meter positioning accuracy in three dimensions. It supports GNSS (GPS/GLONASS) L1 and L2 signals.

The receiver supports differential correction methods including L-Band, RTK, SBAS, and Beacon. The R320 employs innovative Hemisphere GPS Eclipse SureTrack technology, which allows it to model the phase on satellites that the airborne unit is currently tracking. With SureTrack technology, dropouts are reduced and speed of the signal reacquisitions is increased; enhancing accurate positioning when base corrections are not available.

Figure 18: Hemisphere R320 GPS receiver.

4.0 Survey Operations

The survey was flown from August 6 to August 10, 2020 in variable summer conditions. The crew experienced minor delays due to rain, low clouds, and high wind. The experience of the pilot ensured that data quality objectives were met, and that safety of the flight crew was never compromised given the potential risks involved in airborne geophysical surveying. Field processing and quality control checks were performed daily.

4.1 Operations Base and Crew

The base of operation for the Mount Vic survey was at Carmacks airport, Yukon, east of the survey block.

Precision's geophysical crew consisted of four members (Table 2):

Crew Member	Position
Harmen Keyser, P.Geo.	Helicopter pilot
Bruce Larsen	Geophysical operator and helicopter pilot
Shawn Walker, M.Sc., P.Geo.	Geophysicist – data processor and mapping
Jenny Poon, B.Sc., P.Geo.	Geophysicist – data processor, mapping, and reporting

Table 2: List of survey crew members.

4.2 Magnetic Base Station Specifications

Changes in Earth's magnetic field over time, such as diurnal variations, magnetic pulsations, and geomagnetic storms, were measured and recorded by two stationary GEM GSM-19T proton precession magnetometers. The magnetic base stations were installed in an area (Table 3; Figures 19 and 20) of low magnetic noise away from metallic items such as ferromagnetic objects, vehicles, and power lines that could affect the base stations and ultimately the survey data.

Station Name	Easting/Northing	Latitude/Longitude	Datum/Projection
GEM 3 S/N 5081669	392291 m E 6878742 m N	137° 3' 30.17" W 62° 1' 32.20" N	WGS 84, Zone 8N
GEM 4 S/N 2065370	392287 m E 6878740 m N	137° 3' 30.46" W 62° 1' 32.12" N	WGS 84, Zone 8N

Table 3: Magnetic base station locations.

Magnetic readings were reviewed at regular intervals to ensure that no airborne data were collected during periods of high magnetic activity (greater than 10 nT change per minute).

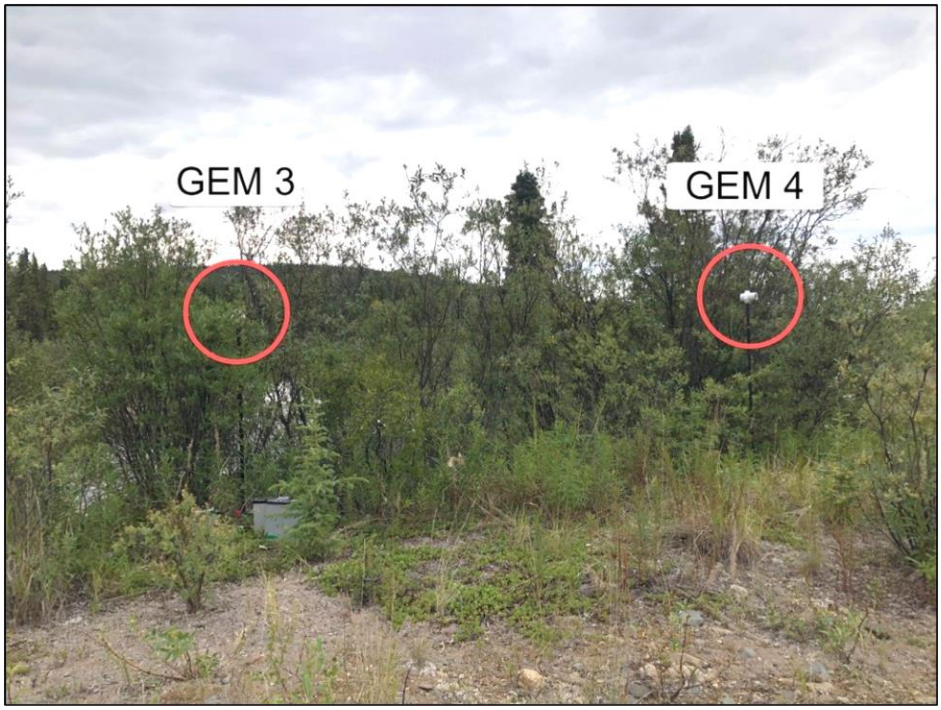

Figure 19: GEM 3 (left) and GEM 4 (right) magnetic base stations at Victoria Creek, Yukon.

Figure 20: Location of GEM 3 (orange) and GEM 4 (green) magnetic base stations at Victoria Creek, Yukon.

4.3 Field Processing and Quality Control

Survey data were transferred from the aircraft's data acquisition system onto a USB memory stick and copied onto a field data processing laptop. The raw data files in PEI binary data format were converted into Geosoft GDB database format. Using Geosoft Oasis Montaj 9.8, the data were inspected to ensure compliance with contract specifications (Table 4; Figures 21 to 23).

Parameter	Specification	Tolerance
Position	Line Spacing	Flight line deviation within 8 m L/R from ideal flight path. No exceedance for more than 1 km.
	Height	Nominal flight height of 40 m above ground level (AGL) with tolerance of ±10 m. No exceedance for more than 1 km, provided deviation is not due to tall trees, topography, mitigation of wildlife/livestock harassment, cultural features, powerlines, railway, or other obstacles beyond the pilot's control.
	GPS	GPS signals from four or more satellites must be received at all times, except where signal loss is due to topography. No exceedance for more than 1 km.
Magnetics	Temporal/Diurnal Variations	Non-linear temporal magnetic variations within 10 nT of a linear chord of length 1 minute.
	Normalized 4th Difference	Magnetic data within 0.02 nT peak to peak. No exceedance for distances greater than 1 km or more, provided noise is not due to geological or cultural features.
Radiometrics	Moisture Conditions	No delays shall be incurred due to unfavourable radiometric survey conditions.

Table 4: Contract survey specifications.

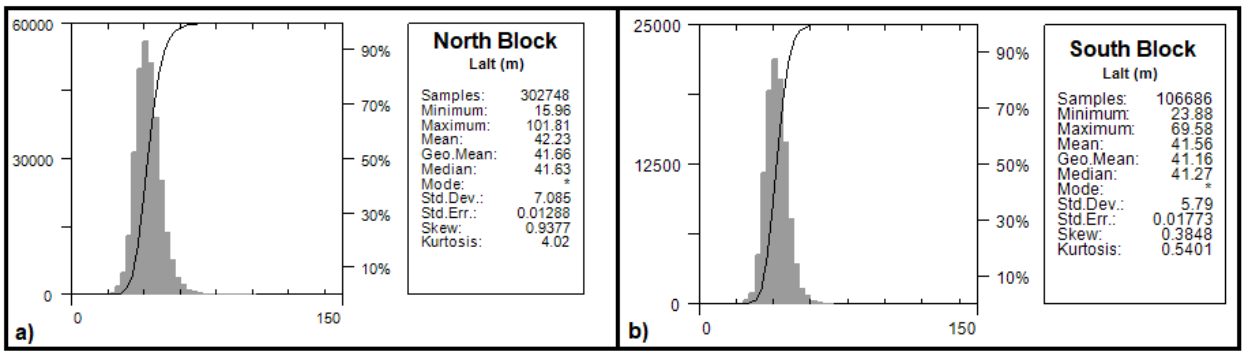

Figure 21: Histogram showing survey elevation vertically above ground. a) North block b) South block.

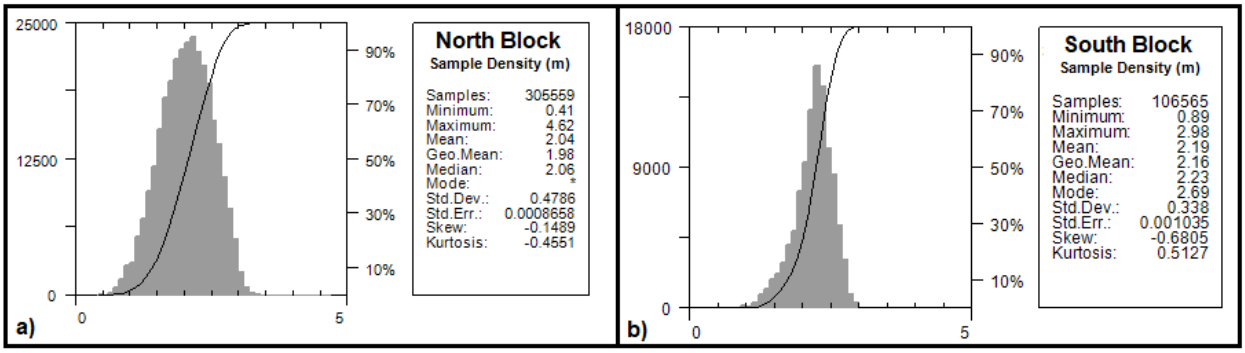

Figure 22: Histogram showing magnetic sample density. Horizontal distance in meters between adjacent measurement locations; magnetic sample frequency 20 Hz. a) North block b) South block.

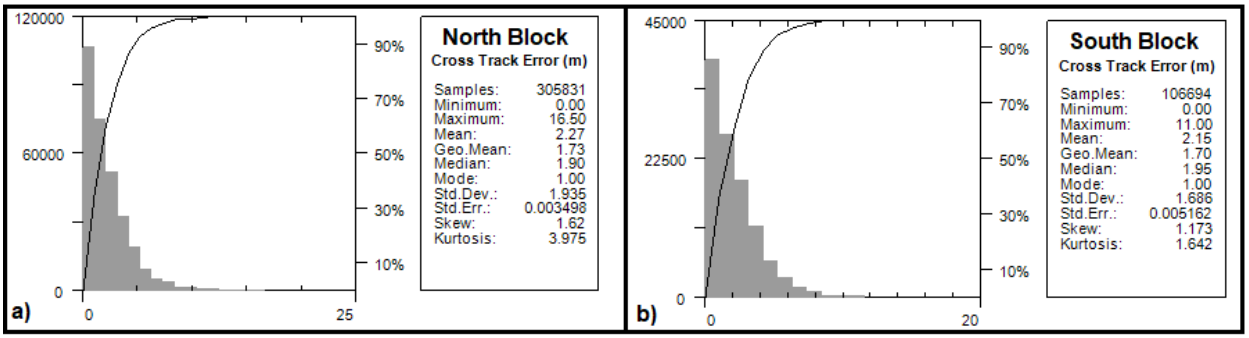

Figure 23: Histogram showing cross track error. a) North block b) South block.

5.0 Data Acquisition Equipment Checks

Airborne equipment tests and calibrations were conducted for the laser altimeter, magnetometer, and spectrometer. A lag test was performed for all three sensors. In addition, there were two tests conducted for the airborne magnetometer: compensation flight and heading error test. There were three tests conducted for the gamma spectrometer: calibration pad test, cosmic flight test, and altitude correction and sensitivity test.

5.1 Lag Test

A lag test was performed to determine the difference in time the digital reading was recorded for the magnetometer, spectrometer, and laser altimeter with the position fix time that the fiducial of the reading was obtained by the GPS system resulting from a combination of system lag and different locations of the various sensors and the GPS antenna. The test was flown in the four orthogonal survey headings over an identifiable magnetic anomaly at survey speed and height. The resulting data (Table 5) were used to correct for time and position.

Instrument	Source	Lag Fiducial	Correction (sec)
Magnetometer	Logging equipment	6	0.30
Spectrometer	Lake edge	32	1.60
Laser Altimeter	Sharp gully	24	1.20

Table 5: Survey lag correction values.

Validity of the lag correction values was confirmed by a lack of offsets (corrugations) in geophysical profiles from adjoining survey lines.

5.2 Magnetometer Tests

The magnetometer was tested and calibrated with a series of dedicated flights specifically for removing undesired effects of aircraft movement, speed, and heading direction.

5.2.1 Compensation Flight Test

During aeromagnetic surveying, a small but significant amount of noise is introduced to the magnetic data by the aircraft itself, as the magnetometer is within the aircraft's magnetic field. Changes in aircraft attitude combined with the permanent magnetization of certain aircraft parts (in particular the engine and other ferrous magnetic objects) contribute to this noise. The aircraft was degaussed using proprietary technology prior to starting the survey and the remaining magnetic noise was removed by a process called magnetic compensation.

A magnetic compensation flight was completed (Table 6) and applied to both survey blocks. The process consists of a series of prescribed maneuvers (±10° roll, ±10° pitch, and ±10° yaw) where the aircraft flies in the four orthogonal headings required (080°/170°/260°/350° in the case of this survey for the two survey blocks) at a sufficient altitude (typically > 2,500 m AGL) in an area of low magnetic gradient where Earth's magnetic field becomes nearly uniform at the scale of the compensation flight. In each heading direction, three specified roll, pitch, and yaw maneuvers (total 36) are performed by the pilot at constant elevation so that any magnetic variation recorded by the airborne magnetometer can be attributed to aircraft movement. These maneuvers are recorded by the airborne fluxgate magnetometer and provide the data that are required to calculate the necessary parameters for compensating the magnetic data to remove aircraft noise from survey data.

Pre-Compensation					Post-Compensation				
Heading	**Roll**	**Pitch**	**Yaw**	**Total**	**Heading**	**Roll**	**Pitch**	**Yaw**	**Total**
080°	0.469	0.4827	0.1937	1.1454	080°	0.0307	0.0375	0.0406	0.1088
170°	0.5573	0.2451	0.2088	1.0112	170°	0.0263	0.0269	0.0254	0.0789
260°	0.3532	0.3010	0.0873	0.7415	260°	0.0407	0.0369	0.0302	0.1078
350°	0.4705	0.6410	0.3118	1.4233	350°	0.0251	0.0307	0.0277	0.0835
Total	1.8500	1.6698	0.8016		**Total**	0.1228	0.1320	0.1239	
FOM (nT) = 4.3214					**FOM (nT) = 0.3787**				

Table 6: Results of compensation flight.

5.2.2 Heading Correction Test

To determine heading errors and other offsets, two cloverleaf pattern flight tests were conducted at high altitude. The cloverleaf tests were flown in the same orthogonal headings as the survey and tie lines (080°/170°/260°/350° and 060°/150°/240°/330° in the case of this survey) at >2500 m AGL in an area with low magnetic gradient. For all four directions the survey helicopter must pass over the same mid-point, at the same elevation, with the aircraft in straight and level flight. The difference in magnetic values obtained in reciprocal headings is the heading error. Heading correction values derived from the test flights are summarized in Tables 7 and 8.

Heading	Fiducial	Mag (nT)	Correction (nT)
080°	98.6	55408.33	-1.9625
170°	351.0	55403.78	2.5875
260°	228.7	55409.51	-3.1425
350°	350.8	55403.85	2.5175
	Average	55329.21	
	Total		0.0000

Table 7: Magnetic sensor heading corrections for the North survey block.

Heading	Fiducial	Mag (nT)	Correction (nT)
060°	572.4	56445.22	-1.4925
150°	356.1	56445.56	-1.8325
240°	466.9	56440.09	3.6375
330°	239.7	56444.04	-0.3125
	Average	56443.7275	
	Total		0.0000

Table 8: Magnetic sensor heading corrections for the South survey block.

5.3 Gamma-ray Spectrometer Tests and Calibrations

Calibration and testing of the RSX-5 airborne gamma-ray spectrometry system was carried out prior to the start of the survey. The calibration of the spectrometer system involved three tests which enabled the conversion of airborne data to ground concentration of natural radioactive elements. These tests were the calibration pad test, cosmic flight test, and the altitude correction and sensitivity test. Measurements were made in accordance with IAEA technical report series No. 323, *Airborne Gamma Ray Spectrometer Surveying*, and AGSO Record 1995/60, *A Guide to the Technical Specifications for Airborne Gamma-Ray Surveys*.

5.3.1 Calibration Pad Test

The calibration pad test was conducted using GSC (Geological Survey of Canada) portable calibration pads. The pads are slabs of concrete containing known concentrations of the radioelements (K, Th, and U) and are used to simulate ideal geological sources of radiation. The measurements collected from the calibration pad test were used to determine Compton scattering and Grasty backscatter (spectral overlap between element windows) coefficients.

5.3.2 Cosmic Flight Test

While the background source of gamma radiation from the aircraft itself is essentially constant, the amount of signal detected from ground sources varies with ground clearance. As the height of the aircraft increases, the distance between the ground and the spectrometer crystals increases, and the proportion of cosmic radiation in each spectral window increases exponentially due to radiation of cosmic origin. The cosmic flight test is conducted to determine the aircraft's background attenuation coefficients for the detector crystal packs and the cosmic coefficients. The pilot is required to fly over the same location repeatedly in opposite directions at 4000, 5000, 6000, 7000, and 8000 feet (1220, 1520, 1830, 2130, and 2440 m) above ground, for approximately 2 minutes each, to collect gamma data used to determine the amount of non-terrestrial signal present in the total gamma signal.

5.3.3 Altitude Correction and Sensitivity Test

The altitude and sensitivity test is similar to the cosmic flight test but is conducted at lower elevations. The aircraft is required to fly over the same location at 30, 40, 50, 70, and 90 m above ground, for two minutes each. As the distance of the aircraft increases above the radioactive ground source, the source signature exponentially degrades. As a result, this test is used to determine the altitude attenuation coefficients and the radio-element sensitivity of the airborne spectrometer system.

6.0 Data Processing

After all data were collected, several procedures were undertaken to ensure that all data met a high standard of quality. All magnetic and radiometric data recorded were converted into Geosoft and ASCII file formats. Further processing (Figure 24) was carried out using Geosoft Oasis Montaj 9.8 geophysical processing software along with proprietary processing algorithms. Laser altimeter, radiometric, and GPS data were resampled to 20 Hz to correspond with the sampling rate of the magnetometer.

6.1 Position Corrections

In order to collect high resolution geophysical data, the location at which the data were measured and recorded must be accurate.

6.1.1 Lag Correction

A correction for lag error was applied to the geophysical data recorded at each individual sensor to compensate for the combination of lag in the recording system and the sensing instrument flying in a different location from the GPS antenna, as determined during the lag test.

6.2 Magnetic Processing

Raw magnetic data, as collected by the airborne instruments, were corrected for aircraft influence, flight maneuvers, temporal variations, lag, and heading. The data were examined for magnetic noise and spikes, which were removed as required. The background magnetic field, International Geomagnetic Reference Field (IGRF) of the Earth, was removed and survey and tie line data of the resulting residual magnetic field were then leveled.

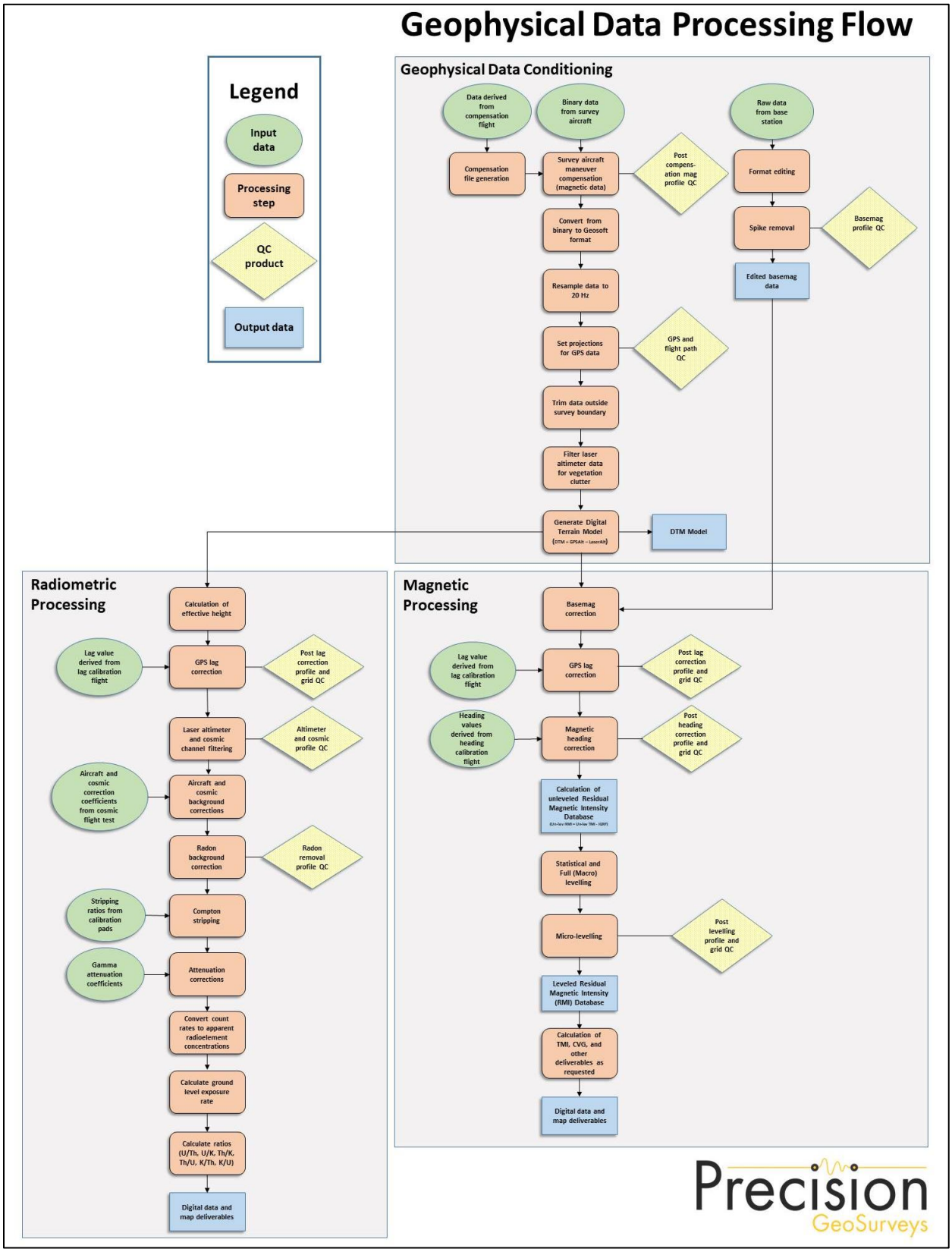

Figure 24: Magnetic and radiometric data processing flow.

6.2.1 Flight Compensation

Data obtained from the compensation flight test were applied to the raw magnetic data as the first step of data processing. A computer program called PEIComp was used to create a model from the compensation flight test for each survey to remove the noise induced by the aircraft and its movement; this model was applied to data from each survey flight.

6.2.2 Temporal Variation Correction

The intensity of Earth's magnetic field varies with location and time. The time variable, known as diurnal or more correctly temporal variation, is removed from the recorded airborne data to provide the desired magnetic field at a specified location. Magnetic data from base station GEM 3 were used for correcting the airborne magnetic survey data, and GEM 4 data were retained for backup. The data were edited, plotted, and merged into a Geosoft database (.GDB) on a daily basis.

Base station measurements from GEM 3 were averaged to establish a magnetic reference datum of 56475.97 nT. Magnetic deviations relative to the reference datum were used to calculate the observed variations of the Earth's magnetic field over time. The airborne magnetic data were then corrected for temporal variations by subtracting base station deviations from data collected on the aircraft, effectively removing effects of diurnal and other temporal variations.

6.2.3 Heading Correction

For each survey heading, changes in instrument magnetic fields along a survey flight line are detected and these systematic shifts are recorded. These values are used to construct a heading table (.TBL) file. An intersection table was created, containing all magnetic field values where tie lines intersected the survey lines and the overall average magnetic field value was calculated. For each of the four headings, the averages were calculated and then compared to the overall average to determine four values to be used for heading error correction in each flight direction.

6.2.4 IGRF Removal

The International Geomagnetic Reference Field (IGRF) model is the empirical representation of Earth's magnetic field (main core field without external sources) collected and disseminated from satellite data and from magnetic observatories around the world. The IGRF has historically been revised and updated every five years by a group of modellers associated with the International Association of Geomagnetism and Aeronomy (IAGA). The 13th generation IGRF (IGRF-13) released in December 2019 was used.

The initial unleveled Residual Magnetic Intensity (RMI) was calculated by taking the difference between IGRF and the non-leveled Total Magnetic Intensity (TMI) to create a more valid model of individual near-surface anomalies. This model is independent of time to allow for other magnetic data (previous or future) to be more easily incorporated into each survey database.

6.2.5 Leveling and Micro-leveling

Residual magnetic intensity (RMI) from survey and tie lines was then used to level the entire survey dataset. Two types of leveling were applied to the corrected data: conventional leveling and micro-leveling. There were two components to conventional leveling: statistical leveling to level tie lines and full leveling to level survey lines. The statistical leveling method corrected the SL/TL intersection errors that follow a specific pattern or trend. Through the error channel, an algorithm calculated a least-squares trend line and derived a trend error curve, which was then added to the channel to be leveled. The second component was full leveling. This adjusted the magnetic value of survey lines so that all lines matched trended tie lines at each intersection point.

Following statistical leveling, micro-leveling was applied to corrected conventional leveled data. This iterative grid-based process removed low amplitude components of flight line noise that still remained after tie line and survey line leveling and resulted in fully leveled RMI data. The IGRF was then added back onto the RMI to allow for the production of a leveled TMI grid and map.

6.2.6 Reduction to Magnetic Pole

Reduced to Magnetic Pole (RTP) data were computed from the leveled Residual Magnetic Intensity (RMI) data. The RTP filter was applied in the Fourier domain and migrates the observed magnetic inclination and declination field to what the field would look like at the north magnetic pole.

Inclination and declination were calculated by using the “Date” channel. The derived values were used in the following formula:

$$RTP\ (\theta) = \frac{[\sin(I) - I\ \cdot \cos(I) \cdot \cos(D-\theta)]^2}{[\sin^2(I_a) + \cos^2(I_a) \cdot \cos^2(D-\theta)] \cdot [\sin^2(I) + \cos^2(I) \cdot \cos^2(D-\theta)]}$$

where: I is geomagnetic inclination in ° from horizontal
D is geomagnetic declination in ° azimuth from magnetic north
I_a is the inclination for amplitude correction (never less than I). Default is +/- 20°. If $|I_a|$is specified to be less than$|I|$, it is set to I

6.2.7 Calculation of Horizontal Gradient

Calculated Horizontal Gradient (CHG) is the magnitude of the total horizontal gradient. It is used to estimate contact locations of magnetic bodies at shallow depths, reveal anomaly texture, and highlight anomaly-pattern discontinuities.

If M is the magnetic field, then the CHG is calculated as:

$$\mathrm{CHG}(x,y) = \sqrt{\left(\frac{\partial M}{\partial x}\right)^2 + \left(\frac{\partial M}{\partial y}\right)^2}$$

6.2.8 Calculation of First Vertical Derivative

The first vertical derivative was computed from the leveled Residual Magnetic Intensity (RMI) data. The first vertical derivative is the vertical rate of change in the magnetic field. It is used to enhance shorter wavelength signals; therefore, edges of magnetic anomalies are highlighted, and deep geologic sources in the data are suppressed.

The first vertical derivative calculated from the RMI was designated as Calculated Vertical Gradient of RMI, or CVG.

The filter, L, used to produce the n^{th} vertical derivative is described by:

$$L(r) = r^n$$

where: r is the radial component in the wavenumber domain

6.3 Radiometric Processing

Radiometric surveys map gamma rays from the concentration of radioelements at or near Earth's surface; typically, up to 1 m below surface. Before airborne radiometric data are processed, the spectrometer system is calibrated with the calibration pad test, cosmic flight test, and altitude correction and sensitivity test. Once calibration of the system was completed, radiometric data were processed by windowing the full spectrum to create individual channels for U, Th, K, and total count (TC).

Steps taken to process acquired radiometric data are summarized below:

- Calculation of effective height
- Aircraft and Cosmic background corrections
- Radon background correction

- Stripping ratios
- Attenuation corrections
- Conversion to apparent radioelement concentrations

6.3.1 Calculation of Effective Height

Laser/Radar altimeter data were converted to effective height (h_{ef}) in meters using laser/radar altimeter, temperature, and pressure data, according to the formula below:

$$h_{ef} = h * \frac{273.15}{T + 273.15} * \frac{P}{1013.25}$$

where: h is observed laser/radar altitude in meters
T is measured air temperature in degrees Celsius
P is barometric pressure in millibars

6.3.2 Aircraft and Cosmic Background Corrections

Aircraft background and cosmic stripping corrections are applied to all three elements, and total count, using the following formula:

$$C_{ac} = \mathrm{a}_c + b_c * Cos_f$$

where: C_{ac} is the background and cosmic corrected channel
a_c is the aircraft background for this channel
b_c is the cosmic stripping coefficient for this channel
Cos_f is the filtered cosmic channel

6.3.3 Radon Background Correction

To strip the effects of atmospheric radon from the downward-looking detectors, there are multiple methods available for radon background estimation. The method selected was the background table method. Procedures to the background table method and how to determine radiometric values filled within the table in detail are outlined in the IAEA 1363 report, *Guidelines for Radioelement Mapping using Gamma Ray Spectrometry Data*.

6.3.4 Compton Stripping

Spectral overlap corrections are applied to potassium, uranium, and thorium as part of the Compton stripping process. This is done by using the stripping ratios that have been calculated for the spectrometer by prior calibration.

For each of the stripping ratios α, β, and γ, they are corrected for height at STP using the following formulas:

$$\alpha_h = \alpha + h_{ef} * 0.00049$$

$$\beta_h = \beta + h_{ef} * 0.00065$$

$$\gamma_h = \gamma + h_{ef} * 0.00069$$

where: $\alpha, \beta,$ and γ are the Compton stripping coefficients
$\alpha_h, \beta_h,$ and γ_h are the height-corrected Compton stripping coefficients
h_{ef} is the effective height above ground in metres at STP

Stripping corrections are then carried out using the following formulas:

$$Th_c = Th_{bc}(1 - g\beta_h) + U_{bc}(b\gamma_h - a) + K_{bc}(ag - b)/A$$

$$U_c = Th_{bc}(g\beta_h - \alpha_h) + U_{bc}(1 - b\beta_h) + K_{bc}(b\alpha_h - g)/A$$

$$K_c = [Th_{bc}(\alpha_h\gamma_h - \beta_h) + U_{bc}(a\beta_h - \gamma_h) + K_{bc}(1 - a\alpha_h)]/A$$

where: $U_c, Th_c,$ and K_c are stripping-corrected uranium, thorium, and potassium
$\alpha_h, \beta_h,$ and γ_h are height-corrected Compton stripping coefficients
$U_{bc}, Th_{bc},$ and K_{bc} are background corrected uranium, thorium, and potassium
a is the spectral ratio Th/U
b is the spectral ratio Th/K
g is the spectral ratio U/K
$A = 1 - g\gamma_h - (\alpha_h - g\beta_h) - b(\beta_h - \alpha_h\gamma_h)$ is the backscatter correction

6.3.5 Attenuation Corrections

Total count, potassium, uranium, and thorium data are then corrected to a nominal survey altitude (corrected to remove vegetation clutter from radar/laser altimeter data); in this case the nominal survey height was 40 m AGL. This is done according to the equation:

$$C_a = C * e^{\mu(h_{ef} - h_0)}$$

where: C_a is the output altitude-corrected channel
C is the input channel
μ is the attenuation correction for that channel
h_{ef} is the effective altitude
h_0 is the nominal survey altitude used as datum

6.3.6 Conversion to Apparent Radioelement Concentrations

With all corrections applied to the radiometric data, the final step is to convert the corrected potassium (^{40}K), uranium (from ^{214}Bi), and thorium (from ^{212}Tl) to apparent radioelement concentrations using the following formula:

$$eE = C_{cor}/S$$

where: eE is the element concentration of K (%) and equivalent element concentration of U (ppm) & Th (ppm)
S is the experimentally determined sensitivity
C_{cor} is the fully corrected channel

Conversion of total count to natural exposure rate (Grasty et al, 1984) is determined by using the following formula:

$$\text{Natural Exposure} = [(1.505 * K) + (0.625 * eU) + (0.31 * eTh)]$$

where: Natural Exposure is in µR/hr
K is the concentration of potassium (%)
eU is the equivalent concentration of uranium (ppm)
eTh is the equivalent concentration of thorium (ppm)

6.3.7 Radiometric Ratios

Common radiometric ratios (U/Th, Th/K, U/K, and their inverses) were calculated using the guidelines of the IAEA. Due to statistical uncertainties in the individual radioelement measurements, care was taken during ratio calculation in order to obtain statistically significant values. The following guidelines were used to determine the ratios:

1. For each concentration, the lowest corrected count rate is determined.
2. Element concentrations of adjacent points on either side of each data point are summed until they exceed a pre-determined threshold value.
3. The ratios are calculated using the accumulated sums.

With these guidelines, errors associated with the calculated ratios are minimized and comparable for all data points.

6.3.8 Ternary Radioelement Image Map

A ternary radioelement image map is a composite colour image that shows each of the primary colours - red (magenta), green, and blue (cyan) - in proportion to radioelement concentration

values of the respective %K, eTh, and eU components. Dark and light colours indicate high and low values for all three radionuclides, respectively. Areas of low radioactivity, and consequently low signal to noise ratios, can be masked and are shaded in white. Because the ternary image is a three-way ratio, it helps to remove topographic and physiographic effects and provides a visualization of the relative concentrations of the individual radioelements.

7.0 Deliverables

Mount Vic data are presented as digital databases, maps, and a logistics report.

7.1 Digital Data

The digital files have been provided in two formats, the first is a .GDB file for use in Geosoft Oasis Montaj and the second format is a text (.XYZ) file. Full descriptions of the digital data and contents are included in the report (Appendix C).

Mount Vic digital data were represented as grids as listed below:

- Digital Terrain Model (DTM)
- Total Magnetic Intensity (TMI)
- Residual Magnetic Intensity (RMI) – removal of IGRF from TMI
- Reduced to Magnetic Pole (RTP) – reduced to magnetic pole of RMI
- Calculated Horizontal Gradient (CHG) – total magnitude of the horizontal gradients of RMI
- Calculated Vertical Gradient (CVG) – first vertical derivative of RMI
- Potassium – Percentage (%K)
- Thorium – Equivalent Concentration (eTh)
- Uranium – Equivalent Concentration (eU)
- Total Count (TC)
- Total Count – Exposure Rate (TCexp)
- Potassium over Thorium Ratio (%K/eTh)
- Potassium over Uranium Ratio (%K/eU)
- Uranium over Thorium Ratio (eU/eTh)
- Uranium over Potassium Ratio (eU/%K)
- Thorium over Potassium Ratio (eTh/%K)
- Thorium over Uranium Ratio (eTh/eU)
- Ternary Image (TI)

7.1.1 Grids

Digital data were gridded and displayed using the following Geosoft parameters:

- Gridding method: minimum curvature

- Grid cell size: 12.5 m
- Low-pass desampling factor: 2
- Tolerance: 0.001
- % pass tolerance: 99.99
- Maximum iterations: 100

All magnetic and radiometric grids were drawn with a histogram-equalized colour shade; sun illumination inclination at 45° and declination at 045°. DTM grid was drawn with a histogram-equalized topographic colour.

7.2 KMZ

Gridded digital data were exported into .KMZ files which can be displayed using Google Earth. The grids can be draped onto topography and rendered to give a 3D view.

7.3 Maps

Digital maps were created for Mount Vic – North and South survey blocks. The following map products were prepared:

Overview Maps (colour images and non-shaded with elevation contour lines and topographic features):

- Actual flight lines
- DTM

Magnetic Maps (colour images with elevation contour lines):

- TMI, with actual flight lines and topographic features
- TMI
- RMI
- RTP of RMI
- CHG of RMI
- CVG of RMI

Radiometric Maps (colour images with elevation contour lines and topographic features):

- %K – Percentage
- eTh – Equivalent Concentration
- eU – Equivalent Concentration
- TC
- TCexp – Exposure Rate
- %K/eTh Ratio

- %K/eU Ratio
- eU/eTh Ratio
- eU/%K Ratio
- eTh/%K Ratio
- eTh/eU Ratio
- Ternary Image

All survey maps were prepared in WGS 84 and UTM Zone 8N.

7.4 Report

A .PDF copy of the logistics report is included along with digital data and maps. The report provides information on data acquisition procedures, data processing, and presentation of the Mount Vic survey data.

8.0 Conclusions and Recommendations

The Mount Vic survey resulted in the collection of 864 line km of high resolution magnetic and radiometric data over two survey blocks. The data have been processed and plotted on maps as a representation of the magnetic and radioactive features of the survey area.

Processing of geophysical data, including the calculation of derivatives, can generate false features as the signal-to-noise ratio decreases. In addition, false features can appear near the edges of a survey block where gridding algorithms are unable to properly calculate grids, such as in "edge effects." Therefore, subtle geophysical features in derivative-enhanced map products or near the survey margins must be evaluated with discretion.

The airborne geophysical data were acquired to map the geophysical characteristics of the survey area, which are in turn related to the distribution and concentration of magnetic minerals and radioactive elements in the Earth. Geophysical data are rarely a direct indication of mineral deposits and therefore interpretation and careful integration with existing and new geological, geochemical, and other geophysical data are recommended to maximize value from the survey investment.

Respectfully submitted,
Precision GeoSurveys Inc.

Jenny Poon, P.Geo.

Appendix A

Polygon Coordinates

Mount Vic – North – WGS 84 Zone 8N

Latitude (deg N)	Longitude (deg W)	Easting (m)	Northing (m)
62.15858	137.24549	383016	6893874
62.16820	137.13999	388546	6894759
62.13465	137.12581	389162	6890998
62.13380	137.13453	388704	6890919
62.11371	137.12599	389076	6888667
62.10835	137.18302	386081	6888169
62.12847	137.19159	385710	6890425
62.12459	137.23085	383648	6890062

Mount Vic – South – WGS 84 Zone 8N

Latitude (deg N)	Longitude (deg W)	Easting (m)	Northing (m)
62.08121	137.23313	383363	6885236
62.09804	137.17165	386636	6887001
62.07623	137.14435	387980	6884525
62.05924	137.20579	384707	6882740

Appendix B

Equipment Specifications

- GEM GSM-19T Proton Precession Magnetometer (Magnetic Base Station)
- Hemisphere R320 GPS Receiver
- Opti-Logic RS800 Rangefinder Laser Altimeter
- Setra Model 276 Barometric Pressure
- Scintrex CS-3 Survey Magnetometer
- Billingsley TFM100G2 Ultra Miniature Triaxial Fluxgate Magnetometer
- Rotronic HygroClip HC-S3 Relative Humidity and Temperature Probe
- Nuvia Dynamics Advanced Gamma-Ray Spectrometer (AGRS)
- Nuvia Dynamics IMPAC data recorder system (for navigation and geophysical data acquisition)

GEM GSM-19T Proton Precession Magnetometer (Magnetic Base Station)

Sensitivity	0.15 nT @ 1 Hz
Resolution	0.01 nT (gamma), magnetic field and gradient
Absolute Accuracy	±0.2 nT @ 1 Hz
Operating Range	20,000 nT to 120,000 nT
Gradient Tolerance	Over 7,000 nT/m
Operating Ranges	Temperature: -40°C to +50°C Battery Voltage: 10.0 V minimum to 15 V maximum Humidity: up to 90% relative, non-condensing
Storage Temperature	-50°C to +50°C
Dimensions	Console: 223 x 69 x 40 mm Sensor Staff: 4 x 450 mm sections Sensor: 170 x 71 mm dia. Weight: console 2.1 kg, sensor and staff assembly 2.2 kg
Integrated GPS	Yes

Hemisphere R320 GPS Receiver Specifications

GPS Sensor	Receiver Type	L1 and L2 RTK with carrier phase	
	Channels	12 L1CA GPS 12 L1P GPS 12 L2P GPS 12 L2C GPS 12 L1 GLONASS (with subscription code) 12 L2 GLONASS (with subscription code) 3 SBAS or 3 additional L1CA GPS	
	Update Rate	10 Hz standard, 20 Hz available	
	Cold Start Time	<60 s	
	Warm Start Time 1	30 s (valid ephemeris)	
	Warm Start Time 2	30 s (almanac and RTC)	
	Hot Start Time	10 s typical (valid ephemeris and RTC)	
	Reacquisition	<1 s	
	Differential Options	SBAS, Autonomous, External RTCM, RTK, OmniSTAR (HP/XP)	
Horizontal Accuracy		RMS (67%)	2DRMS (95%)
	RTK [1, 2]	10 mm + 1 ppm	20 mm + 2 ppm
	OmniSTAR HP [1, 3]	0.1 m	0.2 m
	SBAS (WAAS) [1]	0.3 m	0.6 m
	Autonomous, no SA [1]	1.2 m	2.5 m
L-Band Sensor	Channel	Single channel	
	Frequency Range	1530 MHz to 1560 MHz	
	Satellite Selection	Manual or Automatic (based on location)	
	Startup and Satellite Reacquisition Time	15 seconds typical	
Communications	Serial Ports	2 full duplex RS232	
	Baud Rates	4800 – 115200	
	USB Ports	1 Communications, 1 Flash Drive data storage	
	Correction I/O Protocol	Hemisphere GPS proprietary, RTCM v2.3 (DGPS), RTCM v3 (RTK), CMR, CMR+NMEA 0183, Hemisphere GPS binary	
	Timing Output	1 PPS (HCMOS, active high, rising edge sync, 10 kΩ, 10 pF load)	
	Event Marker Input	HCMOS, active low, falling edge sync, 10 kΩ	
Environmental	Operating Temperature	-40°C to +70°C	
	Storage Temperature	-40°C to +85°C	
	Humidity	95% non-condensing	
Power GPS Sensor	Input Voltage Range	8 to 36 VDC	
	Consumption, RTK	<3.5 W (0.30 A @ 12 VDC typical)	
	Consumption, OmniSTAR	<4.3 W (0.36 A @ 12 VDC typical)	

[1] Depends on multipath environment, number of satellites in view, satellite geometry and ionospheric activity.
[2] Depends also on baseline length.
[3] Requires a subscription from OmniSTAR.

Opti-Logic RS800 Rangefinder Laser Altimeter

Accuracy	±1 m on 1x1 m^2 diffuse target with 50% reflectivity, up to 700 m
Resolution	0.2 m
Communication Protocol	RS232-8, N, 1 ASCII characters
Baud Rate	19200
Data Raw Counts	~200 Hz
Data Calibrated Range	~10 Hz
Data Rate	~200 Hz raw counts for un-calibrated operation; ~10 Hz for calibrated operation (averaging algorithm seeks 8 good readings)
Calibrated Range Units	Feet, Meters, Yards
Laser	Class I (eye-safe), 905 nm ± 10 nm
Power	7 - 9 VDC conditioned required, current draw at full power (~ 1.8 W)
Laser Wavelength	RS100 905 nm ± 10 nm
Laser Divergence	Vertical axis – 3.5 mrad half-angle divergence; Horizontal axis – 1 mrad half-angle divergence; (approximate beam “footprint” at 100 m is 35 cm x 5 cm)
Dimensions	32 x 78 x 84 mm (lens face cross section is 32 x 78 mm)
Weight	<227 g (8 oz)
Casing	RS100/RS400/RS800 units are supplied as OEM modules consisting of an open chassis containing optics and circuit boards. Custom housings can be designed and built on request.

Setra Model 276 Barometric Pressure

Performance	Accuracy RSS[1] (at constant temp)	±0.25% FS[2]
	Non-Linearity (BSFL)	±0.22% FS
	Hysteresis	0.05% FS
	Non-Repeatability	0.05% FS
	Thermal Effects[3]	Compensated range: 0°C to +55°C (+30°F to +130°F) Zero shift (over compensated range): 1% FS Span shift (over compensated range): 1% FS
	Resolution	Infinite, limited only by output noise level (0.0005% FS)
	Time Constant	10 msecs to reach 90% final output with step function pressure input
	Long Term Stability	0.25% FS / 6 months
Environmental	Temperature	Operating[4]: -18°C to +79°C (0°F to +175°F) Storage: -55°C to +121°C (-65°F to +250°F)
	Vibration	2 g from 5 Hz to 500 Hz
	Shock	50 g (Operating, 1/2 sine 10 ms)
	Acceleration	10 g
Electrical	Circuit	3-Wire[5] (Exc, Out, Com)
	Power Consumption	0.20 W (24 VDC)
	Output Impedance	5 Ω
	Output Noise	<200 µV RMS (0 to 100 Hz)

[1] RSS of non-linearity, hysteresis, and non-repeatability.
[2] FS = 300 mb for 800 – 1100 mb range; 500 for 600 – 1100 mb range; and 20 PSI for 0 to 20 PSIA.
[3] Units calibrated at nominal 70°F. Maximum thermal error computed from this datum.
[4] Operating temperature limits of the electronics only. Pressure media temperatures may be considerable higher or lower.
[5] The separate leads for +EXC, -EXC, +Out, -Out are commoned internally. The shield is connected to the case. For best performance, either the -Exc or -Out should be connected to the case. Unit is calibrated at the factory with -Exc connected to the case. The insulation resistance between all signal leads are tied together and case ground is 100 Ω minimum at 25 VDC

Scintrex CS-3 Survey Magnetometer

Operating Principal	Self-oscillating split-beam Cesium Vapor (non-radioactive ^{133}Cs)
Operating Range	15,000 nT to 105,000 nT
Gradient Tolerance	40,000 nT/m
Operating Zones	15° to 75° and 105° to 165°
Hemisphere Switching	a) Automatic b) Electronic control actuated by the control voltage levels (TTL/CMOS) c) Manual
Sensitivity	0.0006 nT √Hz rms
Noise Envelope	Typically 0.002 nT peak to peak, 0.1 to 1 Hz bandwidth
Heading Error	±0.20 nT (inside the optical axis to the field direction angle range 15° to 75° and 105° to 165°)
Absolute Accuracy	<2.5 nT throughout range
Output	a) Continuous signal at the Larmor frequency which is proportional to the magnetic field (proportionality constant 3.49857 Hz/nT) sine wave signal amplitude modulated on the power supply voltage b) Square wave signal at the I/O connector, TTL/CMOS compatible
Information Bandwidth	Only limited by the magnetometer processor used
Sensor Head	Diameter: 63 mm (2.5”) Length: 160 mm (6.3”) Weight: 1.15 kg (2.6 lb)
Sensor Electronics	Diameter: 63 mm (2.5”) Length: 350 mm (13.8”) Weight: 1.5 kg (3.3 lb)
Cable, Sensor to Sensor Electronics	3 m (9’ 8”), lengths up to 5 m (16’ 4”) available
Operating Temperature	-40°C to +50°C
Humidity	Up to 100%, splash proof
Supply Power	24 to 35 VDC
Supply Current	Approx. 1.5 A at start up, decreasing to 0.5 A at 20°C
Power Up Time	Less than 15 minutes at -30°C

Billingsley TFM100G2 Ultra Miniature Triaxial Fluxgate Magnetometer

Axial Alignment	Orthogonality better than ±1°
Input Voltage Options	15 to 34 VDC @ 30 mA
Field Measurement Range Options	±100 µT = ±10 V
Accuracy	±0.75% of full scale (0.5% typical)
Linearity	±0.015% of full scale
Sensitivity	100 µV/nT
Scale Factor Temperature Shift	0.007% full scale/°C
Noise	≤12 pT rms/√Hz @ 1 Hz
Output Ripple	3 mV peak to peak @ 2^{nd} harmonic
Analog Output at Zero Field	±0.025 V
Zero Shift with Temperature	±0.6 nT/°C
Susceptibility to Perming	±8 nT shift with ± 5 Gs applied
Output Impedance	332 Ω ± 5%
Frequency Response	3 dB @ >500 Hz (to >4 kHz wide band)
Over Load Recovery	±5 Gs slew <2 ms
Random Vibration	>20 G rms 20 Hz to 2 kHz
Temperature Range	-55°C to +85°C
Acceleration	>60 G
Weight	100 g
Size	3.51 cm x 3.23 cm x 8.26 cm
Connector	Chassis mounted 9 pin male "D" type

Rotronic HygroClip HC-S3 Relative Humidity and Temperature Probe

Relative Humidity	Operating Range	0 to 100% RH
	Accuracy at 23°C	±1.5% RH
	Output	0 – 1 VDC
	Typical Long-Term Stability	Better than ±1% RH per year
Temperature	Measurement Range	-40°C to +60°C
	Temperature Accuracy	-30°C to +60°C ±0.2°C -50°C to +60°C ±0.6°C (worst case)
	Output	0 – 1 VDC
Power	Supply Voltage	3.5 to 50 VDC (typically powered by data logger's 12 VDC supply)
	Current Consumption	<4 mA
Dimensions	Diameter	1.53 cm (0.60'')
	Length	16.8 cm (6.6'')
	Housing Material	Polycarbonate

Nuvia Dynamics Advanced Gamma-Ray Spectrometer (AGRS)

Crystal Volume	Four 4.2 L NaI(Tl) synthetic downward-looking and one 4.2 L NaI(Tl) upward-looking crystals. Total volume of 21 L
Resolution	256/512/1024 channels
Data Handling	Individual detector processing and calibration
Energy Resolution	< 9% (@ 662 keV)
Differential Non-linearity	< 0.1%
Integral Non-linearity	< 0.01%
Gain Stabilization	Automatic multi-peak on natural radioisotopes
Calibration	Automatic using natural background radiation
Dynamic Input Range	250,000 cps (counts/sec) per detector
Baseline Restoration	Digital Individual Pulse Baseline Restoration (IPBR). The baseline is established for each individual pulse for maximum pulse height accuracy
Sampling Rate	0.1 – 10 secs user defined
Pulse Shaping	Digital Pulse Shaping
Power	9 to 40 VDC, 15 W
Detector Power	3 W per detector
Operating Temperature	-20°C up to +50°C
Downward Shielding	6 mm thick lead plate is used for downward-shielding
Upward Shielding	RayShield® non-radioactive shielding on downward-looking crystals
Spectra	20 keV to 3 MeV (plus cosmic)
System Stabilization	Cold start-up: less than 40 secs on the ground
GPS Connectivity	Time and position synchronization; additional add-on
Weight	~115 kg

Nuvia Dynamics IMPAC data recorder system

(for navigation and geophysical data acquisition)

Functions	Integrated Multi-Parameter Airborne Console (IMPAC) with integrated dual Global Positioning System Receiver (GPS) and all necessary navigation guidance software. Inputs for geophysical sensors - portable gamma ray spectrometer GRS-10/AGRS, MMS4/MMS8 Magnetometer, fluxgate, Totem 2A EM, A/D converter, temperature/humidity probe, barometric pressure probe, and laser/radar altimeter. Output for the multi-parameter PGU (Pilot Guidance Unit)
Display	Monitor display 600 x 800 pixels; customized keypad and operator keyboard. Multi-screen options for real-time viewing of all data inputs, fiducial points, flight line tracking, and GPS channels by operator
Navigation	Pilot/operator navigation guidance. Software supports preplanned survey flight plan, along survey lines, way-points, preplanned drape profile surfaces
Data Sampling	Sensor dependent
Data Synchronization	Synchronized to GPS position. Supports dual GPS
Data File	PEI Binary data format
Storage	80 GB
Software	DATAView: Allows fast data verification and conversion of PEI binary data to Geosoft GBN or ASCII formats MapConvert: For survey preparation, calibration and conversion of maps, and survey plot after data acquisition MagComp: For calculation of magnetic compensation coefficients GRS10/AGRS Calibration: High voltage adjustment, linearity correction coefficients calculation, and communication test support AGIS: Real time data acquisition and navigation system. Displays chart/spectrum view in real-time for fast data Quality Control (QC)
Electrical	Multiple ethernet connections, RS232 serial ports, USB ports, and 16-bit differential analog input channels. It can support up to 4 magnetometer sensors
Power Requirement	24 VDC

Appendix C

Digital File Descriptions

- Magnetic Database Descriptions
- Radiometric Database Descriptions
- Geosoft Grid Descriptions
- Map Descriptions

Magnetic Database:

Abbreviations used in the GDB/XYZ files listed below:

CHANNEL	UNITS	DESCRIPTION
X_WGS84	m	UTM Easting – WGS84 Zone 8N
Y_WGS84	m	UTM Northing – WGS84 Zone 8N
Lat_deg	Decimal degree	Latitude – WGS84
Lon_deg	Decimal degree	Longitude – WGS84
Date	yyyy/mm/dd	Dates of the survey flight(s) – Local
FLT		Flight Line numbers
Line		Line numbers
STL		Number of satellite(s)
GPSfix		1 = non-differential 2 = WAAS/SBAS differential
Heading	degree	Heading of aircraft
GPStime	HH:MM:SS	GPS time (UTC)
Geos_m	m	Geoidal separation
XTE_m	m	Cross track error
Galt	m	GPS height – WGS84 Zone 8N (ASL)
Lalt	m	Laser altimeter readings (AGL)
DTM	m	Digital Terrain Model
Sample_Density	m	Horizontal distance in meters between adjacent measurement locations; sample frequency is 20 Hz
Speed_km_hr	km/hr	Ground speed of aircraft in km/hr
basemag	nT	Base station temporal variation data
IGRF	nT	International Geomagnetic Reference Field, IGRF-13
Declin	Decimal degree	Calculated declination of magnetic field
Inclin	Decimal degree	Calculated inclination of magnetic field
XFg	step	X - fluxgate
YFg	step	Y - fluxgate
ZFg	step	Z - fluxgate
Mag_Head	nT	Total Magnetic Intensity - temporal variation, lag, and heading corrected
TMI	nT	Total Magnetic Intensity - micro-leveled
RMI	nT	Residual Magnetic Intensity - micro-leveled

Radiometric Database:

Abbreviations used in the GDB/XYZ files listed below:

CHANNEL	UNITS	DESCRIPTION
X_WGS84	m	UTM Easting – WGS84 Zone 8N
Y_WGS84	m	UTM Northing – WGS84 Zone 8N
Lat_deg	Decimal degree	Latitude – WGS84
Lon_deg	Decimal degree	Longitude – WGS84
Date	yyyy/mm/dd	Date of the survey flight(s) – Local
FLT		Flight Line numbers
LineNo		Line numbers
STL		Number of satellite(s)
GPStime	HH:MM:SS	GPS time (UTC)
Geos_m	m	Geoidal separation
GPSFix		1 = non-differential 2 = WAAS/SBAS differential
Heading	degree	Heading of the aircraft
XTE_m	m	Cross track error
Galt	m	GPS height – WGS84 Zone 8N (ASL)
Lalt	m	Laser altimeter height (AGL)
DTM	m	Digital Terrain Model
Sample_Density	m	Horizontal distance in metres between adjacent measurement locations; sample frequency is 20 Hz
Speed_km_hr	km/hr	Ground speed of aircraft in km/hr
BaroSTP_kPa	kPa	Barometric altitude (pressure and temperature corrected)
Temp_degC	°C	Air temperature
Press_kPa	kPa	Atmospheric pressure
COSFILT	counts/sec	Spectrometer – Filtered Cosmic
UPUFILT	counts/sec	Spectrometer – Filtered Upward Uranium
Kcor	%	Concentration in Percentage - Potassium
Thcor	ppm	Equivalent Concentration - Thorium
Ucor	ppm	Equivalent Concentration - Uranium
TCcor	nGy/hour	Total Count
TCexp	µR/hour	Exposure Rate
KThratio		Spectrometer –%K/eTh ratio
KUratio		Spectrometer –%K/eU ratio
ThKratio		Spectrometer – eTh/%K ratio
ThUratio		Spectrometer – eTh/eU ratio
UKratio		Spectrometer – eU/%K ratio
UThratio		Spectrometer – eU/eTh ratio

Grids:

Mount Vic – North, WGS 84 Datum, Zone 8N, cell size at 12.5 m

FILE NAME	DESCRIPTION
20138_MntVic_North_DTM_12.5m.grd	Digital Terrain Model gridded at 12.5 m cell size
20138_MntVic_North_TMI_12.5m.grd	Total Magnetic Intensity gridded at 12.5 m cell size
20138_MntVic_North_RMI_12.5m.grd	Residual Magnetic Intensity gridded at 12.5 m cell size
20138_MntVic_North_RTP_12.5m.grd	Reduced to Magnetic Pole of RMI gridded at 12.5 m cell size
20138_MntVic_North_CHG_12.5m.grd	Calculated Horizontal Gradient of RMI gridded at 12.5 m cell size
20138_MntVic_North_CVG_12.5m.grd	Calculated Vertical Gradient of RMI gridded at 12.5 m cell size
20138_MntVic_North_K_12.5m.grd	Potassium (%K) – in percentage gridded at 12.5 m cell size
20138_MntVic_North_eTh_12.5m.grd	Thorium (eTh) – equivalent concentration gridded at 12.5 m cell size
20138_MntVic_North_eU_12.5m.grd	Uranium (eU) – equivalent concentration gridded at 12.5 m cell size
20138_MntVic_North_TC_12.5m.grd	Total Count (TC) gridded at 12.5 m cell size
20138_MntVic_North_TCexp_12.5m.grd	Total Count (TCexp) – exposure rate gridded at 12.5 m cell size
20138_MntVic_North_KThratio_12.5m.grd	Potassium over Thorium ratio (%K/eTh) gridded at 12.5 m cell size
20138_MntVic_North_KUratio_12.5m.grd	Potassium over Uranium ratio (%K/eU) gridded at 12.5 m cell size
20138_MntVic_North_UThratio_12.5m.grd	Uranium over Thorium ratio (eU/eTh) gridded at 12.5 m cell size
20138_MntVic_North_UKratio_12.5m.grd	Uranium over Potassium ratio (eU/%K) gridded at 12.5 m cell size
20138_MntVic_North_ThKratio_12.5m.grd	Thorium over Potassium ratio (eTh/%K) gridded at 12.5 m cell size
20138_MntVic_North_ThUratio_12.5m.grd	Thorium over Uranium ratio (eTh/eU) gridded at 12.5 m cell size

Grids:

Mount Vic – South, WGS 84 Datum, Zone 8N, cell size at 12.5 m

FILE NAME	DESCRIPTION
20138_MntVic_South_DTM_12.5m.grd	Digital Terrain Model gridded at 12.5 m cell size
20138_MntVic_South_TMI_12.5m.grd	Total Magnetic Intensity gridded at 12.5 m cell size
20138_MntVic_South_RMI_12.5m.grd	Residual Magnetic Intensity gridded at 12.5 m cell size
20138_MntVic_South_RTP_12.5m.grd	Reduced to Magnetic Pole of RMI gridded at 12.5 m cell size
20138_MntVic_South_CHG_12.5m.grd	Calculated Horizontal Gradient of RMI gridded at 12.5 m cell size
20138_MntVic_South_CVG_12.5m.grd	Calculated Vertical Gradient of RMI gridded at 12.5 m cell size
20138_MntVic_South_K_12.5m.grd	Potassium (%K) – in percentage gridded at 12.5 m cell size
20138_MntVic_South_eTh_12.5m.grd	Thorium (eTh) – equivalent concentration gridded at 12.5 m cell size
20138_MntVic_South_eU_12.5m.grd	Uranium (eU) – equivalent concentration gridded at 12.5 m cell size
20138_MntVic_South_TC_12.5m.grd	Total Count (TC) gridded at 12.5 m cell size
20138_MntVic_South_TCexp_12.5m.grd	Total Count (TCexp) – exposure rate gridded at 12.5 m cell size
20138_MntVic_South_KThratio_12.5m.grd	Potassium over Thorium ratio (%K/eTh) gridded at 12.5 m cell size
20138_MntVic_South_KUratio_12.5m.grd	Potassium over Uranium ratio (%K/eU) gridded at 12.5 m cell size
20138_MntVic_South_UThratio_12.5m.grd	Uranium over Thorium ratio (eU/eTh) gridded at 12.5 m cell size
20138_MntVic_South_UKratio_12.5m.grd	Uranium over Potassium ratio (eU/%K) gridded at 12.5 m cell size
20138_MntVic_South_ThKratio_12.5m.grd	Thorium over Potassium ratio (eTh/%K) gridded at 12.5 m cell size
20138_MntVic_South_ThUratio_12.5m.grd	Thorium over Uranium ratio (eTh/eU) gridded at 12.5 m cell size

Maps:

Mount Vic - North, WGS 84 Datum, Zone 8N (jpegs, pdfs, and georeferenced pdf)

Plate Number	Plate Name	FILE NAME	DESCRIPTION
1_N	FL	20138_MntVic_North_ActualFlightLines	Plotted actual flown flight lines
2_N	DTM	20138_MntVic_North_DTM_12.5m	Digital Terrain Model gridded at 12.5 m cell size
3_N	TMI_wFL	20138_MntVic_North_TMI_wFL_12.5m	Total Magnetic Intensity gridded at 12.5 m cell size with actual flown flight lines
4_N	TMI	20138_MntVic_North_TMI_12.5m	Total Magnetic Intensity gridded at 12.5 m cell size
5_N	RMI	20138_MntVic_North_RMI_12.5m	Residual Magnetic Intensity gridded at 12.5 m cell size
6_N	RTP	20138_MntVic_North_RTP_12.5m	Reduced to Magnetic Pole of RMI gridded at 12.5 m cell size
7_N	CHG	20138_MntVic_North_CHG_12.5m	Calculated Horizontal Gradient of RMI gridded at 12.5 m cell size
8_N	CVG	20138_MntVic_North_CVG_12.5m	Calculated Vertical Gradient of RMI gridded at 12.5 m cell size
9_N	%K	20138_MntVic_North_K_12.5m	Potassium (%K) – in percentage gridded at 12.5 m cell size
10_N	eTh	20138_MntVic_North_eTh_12.5m	Thorium (eTh) – equivalent concentration gridded at 12.5 m cell size
11_N	eU	20138_MntVic_North_eU_12.5m	Uranium (eU) – equivalent concentration gridded at 12.5 m cell size
12_N	TC	20138_MntVic_North_TC_12.5m	Total Count (TC) gridded at 12.5 m cell size
13_N	TCexp	20138_MntVic_North_TCexp_12.5m	Total Count (TCexp) – exposure rate gridded at 12.5 m cell size
14_N	%K/eTh	20138_MntVic_North_KThRatio_12.5m	Potassium over Thorium ratio (%K/eTh) gridded at 12.5 m cell size
15_N	%K/eU	20138_MntVic_North_KURatio_12.5m	Potassium over Uranium ratio (%K/eU) gridded at 12.5 m cell size
16_N	eU/eTh	20138_MntVic_North_UThRatio_12.5m	Uranium over Thorium ratio (eU/eTh) gridded at 12.5 m cell size
17_N	eU/%K	20138_MntVic_North_UKRatio_12.5m	Uranium over Potassium ratio (eU/%K) gridded at 12.5 m cell size
18_N	eTh/%K	20138_MntVic_North_ThKRatio_12.5m	Thorium over Potassium ratio (eTh/%K) gridded at 12.5 m cell size
19_N	eTh/eU	20138_MntVic_North_ThURatio_12.5m	Thorium over Uranium ratio (eTh/eU) gridded at 12.5 m cell size
20_N	TI	20138_MntVic_North_TernaryImage_12.5m	Displaying ratios of all three elements (%K, eTh, eU) gridded at 12.5 m cell size

Maps:

Mount Vic - South, WGS 84 Datum, Zone 8N (jpegs, pdfs, and georeferenced pdf)

Plate Number	Plate Name	FILE NAME	DESCRIPTION
1_S	FL	20138_MntVic_South_ActualFlightLines	Plotted actual flown flight lines
2_S	DTM	20138_MntVic_South_DTM_12.5m	Digital Terrain Model gridded at 12.5 m cell size
3_S	TMI_wFL	20138_MntVic_South_TMI_wFL_12.5m	Total Magnetic Intensity gridded at 12.5 m cell size with actual flown flight lines
4_S	TMI	20138_MntVic_South_TMI_12.5m	Total Magnetic Intensity gridded at 12.5 m cell size
5_S	RMI	20138_MntVic_South_RMI_12.5m	Residual Magnetic Intensity gridded at 12.5 m cell size
6_S	RTP	20138_MntVic_South_RTP_12.5m	Reduced to Magnetic Pole of RMI gridded at 12.5 m cell size
7_S	CHG	20138_MntVic_South_CHG_12.5m	Calculated Horizontal Gradient of RMI gridded at 12.5 m cell size
8_S	CVG	20138_MntVic_South_CVG_12.5m	Calculated Vertical Gradient of RMI gridded at 12.5 m cell size
9_S	%K	20138_MntVic_South_K_12.5m	Potassium (%K) – in percentage gridded at 12.5 m cell size
10_S	eTh	20138_MntVic_South_eTh_12.5m	Thorium (eTh) – equivalent concentration gridded at 12.5 m cell size
11_S	eU	20138_MntVic_South_eU_12.5m	Uranium (eU) – equivalent concentration gridded at 12.5 m cell size
12_S	TC	20138_MntVic_South_TC_12.5m	Total Count (TC) gridded at 12.5 m cell size
13_S	TCexp	20138_MntVic_South_TCexp_12.5m	Total Count (TCexp) – exposure rate gridded at 12.5 m cell size
14_S	%K/eTh	20138_MntVic_South_KThRatio_12.5m	Potassium over Thorium ratio (%K/eTh) gridded at 12.5 m cell size
15_S	%K/eU	20138_MntVic_South_KURatio_12.5m	Potassium over Uranium ratio (%K/eU) gridded at 12.5 m cell size
16_S	eU/eTh	20138_MntVic_South_UThRatio_12.5m	Uranium over Thorium ratio (eU/eTh) gridded at 12.5 m cell size
17_S	eU/%K	20138_MntVic_South_UKRatio_12.5m	Uranium over Potassium ratio (eU/%K) gridded at 12.5 m cell size
18_S	eTh/%K	20138_MntVic_South_ThKRatio_12.5m	Thorium over Potassium ratio (eTh/%K) gridded at 12.5 m cell size
19_S	eTh/eU	20138_MntVic_South_ThURatio_12.5m	Thorium over Uranium ratio (eTh/eU) gridded at 12.5 m cell size
20_S	TI	20138_MntVic_South_TernaryImage_12.5m	Displaying ratios of all three elements (%K, eTh, eU) gridded at 12.5 m cell size

Plates

Mount Vic - North
Scale 1:15,000
(Print and Digital)

- Plate 1_N: Mount Vic - North – Actual Flight Lines (FL)
- Plate 2_N: Mount Vic - North – Digital Terrain Model (DTM)
- Plate 3_N: Mount Vic - North – Total Magnetic Intensity with Actual Flight Lines (TMI_wFL)
- Plate 4_N: Mount Vic - North – Total Magnetic Intensity (TMI)
- Plate 5_N: Mount Vic - North – Residual Magnetic Intensity (RMI)
- Plate 6_N: Mount Vic - North – Reduced to Magnetic Pole (RTP) of RMI
- Plate 7_N: Mount Vic - North – Calculated Horizontal Gradient (CHG) of RMI
- Plate 8_N: Mount Vic - North – Calculated Vertical Gradient (CVG) of RMI
- Plate 9_N: Mount Vic - North – Potassium - Percentage (%K)
- Plate 10_N: Mount Vic - North – Thorium - Equivalent Concentration (eTh)
- Plate 11_N: Mount Vic - North – Uranium - Equivalent Concentration (eU)
- Plate 12_N: Mount Vic - North – Total Count (TC)
- Plate 13_N: Mount Vic - North – Total Count - Exposure Rate (TCexp)
- Plate 14_N: Mount Vic - North – Potassium over Thorium Ratio (%K/eTh)
- Plate 15_N: Mount Vic - North – Potassium over Uranium Ratio (%K/eU)
- Plate 16_N: Mount Vic - North – Uranium over Thorium Ratio (eU/eTh)
- Plate 17_N: Mount Vic - North – Uranium over Potassium Ratio (eU/%K)
- Plate 18_N: Mount Vic - North – Thorium over Potassium Ratio (eTh/%K)
- Plate 19_N: Mount Vic - North – Thorium over Uranium Ratio (eTh/eU)
- Plate 20_N: Mount Vic - North – Ternary Image (TI)

Plates

Mount Vic - South
Scale 1:15,000
(Print and Digital)

- Plate 1_S: Mount Vic - South – Actual Flight Lines (FL)
- Plate 2_S: Mount Vic - South – Digital Terrain Model (DTM)
- Plate 3_S: Mount Vic - South – Total Magnetic Intensity with Actual Flight Lines (TMI_wFL)
- Plate 4_S: Mount Vic - South – Total Magnetic Intensity (TMI)
- Plate 5_S: Mount Vic - South – Residual Magnetic Intensity (RMI)
- Plate 6_S: Mount Vic - South – Reduced to Magnetic Pole (RTP) of RMI
- Plate 7_S: Mount Vic - South – Calculated Horizontal Gradient (CHG) of RMI
- Plate 8_S: Mount Vic - South – Calculated Vertical Gradient (CVG) of RMI
- Plate 9_S: Mount Vic - South – Potassium - Percentage (%K)
- Plate 10_S: Mount Vic - South – Thorium - Equivalent Concentration (eTh)
- Plate 11_S: Mount Vic - South – Uranium - Equivalent Concentration (eU)
- Plate 12_S: Mount Vic - South – Total Count (TC)
- Plate 13_S: Mount Vic - South – Total Count - Exposure Rate (TCexp)
- Plate 14_S: Mount Vic - South – Potassium over Thorium Ratio (%K/eTh)
- Plate 15_S: Mount Vic - South – Potassium over Uranium Ratio (%K/eU)
- Plate 16_S: Mount Vic - South – Uranium over Thorium Ratio (eU/eTh)
- Plate 17_S: Mount Vic - South – Uranium over Potassium Ratio (eU/%K)
- Plate 18_S: Mount Vic - South – Thorium over Potassium Ratio (eTh/%K)
- Plate 19_S: Mount Vic - South – Thorium over Uranium Ratio (eTh/eU)
- Plate 20_S: Mount Vic - South – Ternary Image (TI)